

THE SUPERLUMINOUS (TYPE I) SUPERNOVA ASASSN-15LH: A CASE FOR A QUARK-NOVA INSIDE AN OXYGEN-TYPE WOLF-RAYET SUPERNOVA REMNANT

RACHID OUYED, DENIS LEAHY, LUIS WELBANKS, NICHOLAS KONING

Department of Physics & Astronomy, University of Calgary, 2500 University Drive NW, Calgary, AB T2N 1N4, Canada

Draft version July 28, 2018

ABSTRACT

We show that a Quark-Nova (QN; the explosive transition of a neutron star to a quark star) occurring a few days following the supernova explosion of an Oxygen-type Wolf-Rayet (WO) star can account for the intriguing features of ASASSN-15lh, including its extreme energetics, its double-peaked light-curve and the evolution of its photospheric radius and temperature. A two-component configuration of the homologously expanding WO remnant (an extended envelope and a compact core) is used to harness the kinetic energy ($> 10^{52}$ ergs) of the QN ejecta. The delay between the WO SN and the QN yields a large ($\sim 10^4 R_{\odot}$) envelope which when energized by the QN ejecta/shock gives the first peak in our model. As the envelope's photosphere recedes into the slowly expanding, hot and insulated, denser core (initially heated by the QN shock) a second hump emerges. The spectrum in our model should reflect the composition of an WO SN remnant re-heated by a QN going off in its wake.

Subject headings: Circum-stellar matter – stars: evolution – stars: outflows – supernovae: general – supernovae: individual (ASASSN-15lh)

1. INTRODUCTION

Super-luminous, H-poor, supernovae (SLSNe-I) show peak luminosities that are more than an order of magnitude higher than that of Type-Ia SNe and that of other types of core-collapse SNe (e.g. Pastorello et al. 2010; Quimby et al. 2011; Inserra et al. 2013; Nicholl et al. 2014); see also Gal-Yam 2012 for a review). Suggested explanations include powering by black hole accretion (Dexter & Kasen 2013), millisecond magnetars (Woosley 2010; Kasen & Bildsten 2010), jet energy input (Gilkis et al. 2016), sub-millisecond strange quark stars (Dai et al. 2016)), tidal disruption of a star by a supermassive BH (Leloudas et al. 2016), pulsational pair-instability progenitor models (Kozyreva & Blinnikov 2015; Chatzopoulos et al. 2015) as well as models involving the interaction of SN ejecta with its surroundings (Wang et al. 2015; Moriya et al. 2015; Sorokina et al. 2015; Piro 2015; Dessart et al. 2015). Following the discovery of the most luminous of them all, ASASSN-15lh (Dong et al. 2016), the proposed models have been challenged and pushed to their limits because of the high energy and re-brightening of ASASSN-15lh (Brown et al. 2016; e.g. discussion in Chatzopoulos et al. 2016). It is safe to say that the exact mechanism powering SLSNe-I remains unknown, leaving room for novel ideas to be explored.

The QN model for SLSNe appeals to the explosive transition of a neutron star (NS) to a quark star (QS; the QN compact remnant) a few days following the SN explosion. The extended envelope means that PdV losses are minimal when it is shocked by the QN ejecta yielding a SLSN. This can be the case if the SN explosion of a single massive progenitor is followed a few days later by a QN (Leahy & Ouyed 2008; Ouyed et al. 2009, 2012; Kostka et al. 2014a). A NS in-spiralling inside a Common Envelope in massive binaries gives a similar scenario and if the NS goes QN a SLSN-I results since the hydrogen has been lost during the binary evolution (Ouyed et al. 2015a,b, 2016). We find that ASASSN-15lh is best explained if we consider a QN occurring a few days fol-

lowing the SN explosion of a stripped oxygen sequence Wolf-Rayet star (i.e. an WO-type; Barlow & Hummer 1982). A QN going off in a two-component configuration WO SN remnant (SNR) which consists of a core (a dense, inner region) and an envelope (the extended lower density outer layers) seems to account for the general properties of ASASSN-15lh's lightcurve. The time delay between the QN and the preceding SN means that the QN energy is deposited in a very extended WO SN envelope. When shocked by the QN ejecta, the envelope yields the first hump while the second hump results from the late and slower contribution of the denser inner region (i.e. the core; initially energized by the QN shock; see Figure 1 for illustration purposes). The heated core remains insulated (effectively acting as a “hot plate”) until it is revealed by the receding photosphere of the QN-shocked envelope. Our model reproduces the light-curve of ASASSN-15lh and the evolution of its photospheric radius and temperature. The spectrum in our model should represent the composition of the WO SNR re-heated by the QN shock. In §2, we start with a brief overview of the physics of the QN and of its ejecta followed by a description of the WO SN progenitor it collides with. The method we use to compute the light-curve and the properties of the photosphere is given in §3. We end with a discussion and a conclusion in §4.

2. THE QN IN THE WAKE OF AN WO SN REMNANT

2.1. The QN energetics

Assuming that matter made of up, down and strange quarks is more stable than hadronic matter (Bodmer 1971; Witten 1984), the explosive conversion of a NS to a quark star (QS) remains an intriguing possibility. Theoretical and numerical studies have shown that such a transition is not unlikely (e.g. Dai et al. 1995; Cheng & Dai 1996; Horvath & Benvenuto 1988; Ouyed et al. 2002; Keränen et al. 2005; Niebergal et al. 2010; Herzog & Röpke 2011; Pagliara et al. 2013; Furusawa et al. 2015a,b; Drago & Pagliara 2015a). These studies find

three possible paths to the explosion including, neutrino-driven explosion mechanisms (Keränen et al. 2005; Drago & Pagliara 2015b), photon-driven explosions (Vogt et al. 2004; Ouyed et al. 2005) and quark-core-collapse driven explosion plausibly induced by deleptonization instabilities (Niebergal et al. 2010; see Ouyed, Niebergal & Jaikumar 2013 for a recent review). More sophisticated simulations are required to better capture the micro-physics and macro-physics of the transition. Until then, one may hope for direct and/or indirect observation of the QN to confirm the transition. Here, as in some of our previous work, we assume that the transition is triggered when deconfinement of neutrons to quarks happens inside a massive NS. This may be the case here, if for example, fallback material from the preceding WO SN drives the NS’s mass above the critical value for quark deconfinement. When combined with strange-quark seeding inside the deconfined core, ignition and a conversion “flame” can be fuelled (see Niebergal et al. 2010). For a NS of mass M_{NS} , a QN can release at least $(M_{\text{NS}}/m_{\text{p}})E_{\text{conv.}} \sim 10^{53}$ ergs from the direct conversion of its hadrons to quarks with up to $E_{\text{conv.}} \sim 100$ MeV of energy released per hadron converted (e.g. Weber 2005); m_{p} is the proton mass. Accounting for gravitational energy from contraction and additional energy release during phase transitions within the quark phase (e.g. Vogt et al. 2004), the total energy can reach a few times 10^{53} ergs. The amount imparted as kinetic energy ($E_{\text{QN}}^{\text{KE}}$) to the NS outer layers ($\sim 10^{-3}M_{\odot}$) exceeds $\sim 10^{52}$ ergs (e.g. Keränen et al. 2005). The QN ejecta is a very dense, neutron-rich, relativistic material expanding away from the explosion point at a Lorentz factor > 10 (Jaikumar et al. 2007; Ouyed & Leahy 2009; Kostka et al. 2014b).

2.2. The WO supernova remnant

The extensive mass-loss (of hydrogen and helium) experienced by Wolf-Rayet stars unveils the products of He-burning (${}^8\text{Be}$, ${}^{12}\text{C}$, ${}^{16}\text{O}$) at the stellar surface with the Oxygen-type stars showing much more oxygen than Carbon-type (e.g. Barlow & Hummer 1982). Consider an WO star that just experienced a SN event (panels A & B in Figure 1). If we define M_{WO} as the remnant’s mass and $E_{\text{SN}}^{\text{KE}}$ as the ejecta’s kinetic energy, then for a homologously expanding, uniform density, ejecta the expansion velocity is $v_{\text{SN}} = \sqrt{(10/3)E_{\text{SN}}^{\text{KE}}/M_{\text{WO}}}$. To simplify our model, we assume that the remnant consists of a core of mass M_{core} and an envelope of mass $M_{\text{env.}} = M_{\text{WO}} - M_{\text{core}}$. Defining t_{delay} as the time delay between the SN explosion and the QN explosion, the size of the WO SN remnant when the QN goes off is $R_{\text{env.,0}} = R_{\text{WO}} + v_{\text{SN}}t_{\text{delay}} \simeq v_{\text{SN}}t_{\text{delay}}$ for a SN ejecta expanding at speed v_{SN} with R_{WO} being the radius of the WO-type progenitor star which is negligible ($R_{\text{WO}} \ll R_{\text{env.,0}}$).

Once the QN goes off (panels C in Figure 1), its extremely dense and relativistic ejecta catches up very quickly with the preceding SN ejecta. For example for a typical SN expansion speed of 10^4 km s $^{-1}$ and a time delay of, say, 10 days between the SN and the QN explosion the two ejecta collide after only a fraction of an hour following the QN explosion; i.e. $v_{\text{SN}}t_{\text{delay}}/c \ll t_{\text{delay}}$ where c is the speed of light. In reality, the QN ejecta hits the inner edge of the SN ejecta even much sooner

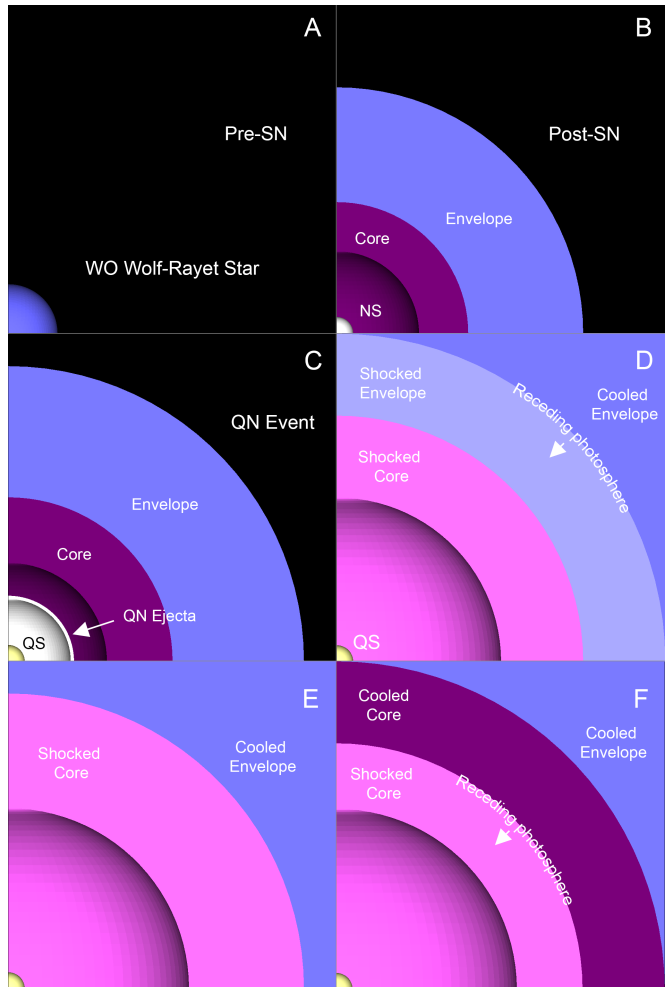


FIG. 1.— Sequence of events in our model starting with the SN explosion of a WO-type star (panels A & B). Panel B depicts the homologously expanding SN ejecta a few days later (just before the QN event) which consists of a dense core and an overlaying extended, and much lower density, envelope. The QN goes off (panel C) leaving behind a QS (the compact remnant) and generating a very dense, relativistic ejecta, which shocks the WO SN remnant. The core is shocked first and then the envelope which starts to radiate and cool as portrayed by its receding photosphere (panel D). The buried core is eventually unveiled (panel E) triggering radiation escape directly from the core giving us the second hump in our model (panel F).

since the speed of the inner SN ejecta is very small.

The QN shock is radiative owing to the low density of the envelope meaning that most of the QN energy is converted to thermal (gas and radiation) and only a small portion is in the form of kinetic energy. In this case, the envelope expansion velocity after the QN shock is effectively that of the SN or, $v_{\text{env.}} = v_{\text{SN}}$. This also implies that the shock velocity in the envelope is given as $v_{\text{env.,sh.}} = (7/6)v_{\text{SN}}$. As the shock makes its way through the large WO SN remnant, part of the QN kinetic energy $E_{\text{QN}}^{\text{KE}}$ is converted to thermal energy in the core (E_{core}) and the remaining ($E_{\text{env.}} = E_{\text{QN}}^{\text{KE}} - E_{\text{core}}$) is used up in the envelope. The QN shock propagating in the envelope (we refer to it as the outer QN-shock) provides the first energy source as it heats up the envelope while the QN shock which propagated in the core (we refer to it as the inner QN-shock) heats up the core. The radiation from

these two energy sources first diffuses in the envelope (panel D in Figure 1) and later in the core (panels E & F in Figure 1) yielding the double-hump nature of the light-curve in ASASSN-15lh as described in the next section. Finally, the SN explosion leads to oxygen- and carbon-burning products in the denser hotter layers of the WO star; i.e. in the core. All of carbon and oxygen should be preserved in the outer layers (i.e. in the envelope). A radiative QN shock is unlikely to alter the chemical composition in the WO SNR which should be reflected in the spectrum according to our model.

3. THE LIGHT-CURVE IN OUR MODEL

3.1. Diffusion in the envelope

To simulate diffusion in the envelope, we integrate Eq. (3) in Chatzopoulos et al. (2012) using a ‘top-hat’ prescription as described in §3.2.1 in that paper. In our case, since we have two sources contributing to the envelope the input luminosity function is given as

$$L_{\text{env.,input}} = \begin{cases} L_{\text{env.,sh.}} + L_{\text{core}}, & \text{if } t \leq t_{\text{env.,sh.}} \\ L_{\text{core}}, & \text{if } t_{\text{env.,sh.}} < t \leq t_{\text{core,sh.}} \\ 0, & \text{otherwise} \end{cases} \quad (1)$$

The QN shock input luminosity into the envelope is $L_{\text{env.,sh.}} = E_{\text{env.}}/t_{\text{env.,sh.}}$ for $t < t_{\text{env.,sh.}}$ and $L_{\text{env.,sh.}} = 0$ otherwise. The shock duration $t_{\text{env.,sh.}}$ is the time it would take the QN shock to traverse the envelope and break-out. It is given as $t_{\text{env.,sh.}} = (R_{\text{env.,0}} + v_{\text{SN}}t_{\text{env.,sh.}})/v_{\text{env.,sh.}}$. This gives $t_{\text{env.,sh.}} = 6R_{\text{env.,0}}/v_{\text{SN}} \simeq 6t_{\text{delay}}$ since $R_{\text{env.,0}} = R_{\text{WO}} + v_{\text{SN}}t_{\text{delay}} \simeq v_{\text{SN}}t_{\text{delay}}$.

The core (first shocked by the QN ejecta) is embedded deep in the envelope and is insulated radiating at a lower and slower rate than the outer shock. It effectively acts as a ‘hot plate’ with an input luminosity into the envelope given by $L_{\text{core,sh.}} = E_{\text{core}}/t_{\text{core,sh.}}$. The time $t_{\text{core,sh.}}$ corresponds to when the envelope’s photosphere recedes deep enough to cross the core radius. For $t > t_{\text{core,sh.}}$, the envelope is optically thin to the radiation from the core and diffusion switches into core diffusion. The input luminosity is that from the core for $t_{\text{env.,sh.}} < t < t_{\text{core,sh.}}$ while the input luminosity from the outer shock dominates mainly at $t < t_{\text{env.,sh.}}$. This is also reflected in the output luminosity. The time $t_{\text{core,sh.}}$ is derived self-consistently in our model as explained in §3.2 below.

The characteristic or effective LC timescale in the envelope (not to be confused with diffusion timescale; see Eq. (3) in Chatzopoulos et al. 2012) is $t_{\text{env.,d}} = \sqrt{2\kappa_{\text{env.}}M_{\text{env.}}/(\beta cv_{\text{SN}})}$ with $\kappa_{\text{env.}}$ the mean opacity in the envelope, $\beta = 13.8$ (Arnett 1980, 1982) and c the speed of light. The corresponding photospheric radius is derived using $R_{\text{env.,ph.}} = R_{\text{env.}}(t) - \alpha_{\lambda}\lambda_{\text{env.}}(t) = (R_{\text{env.,0}} + v_{\text{SN}}t) - \alpha_{\lambda}\lambda_{\text{env.}}(t)$ where $\lambda_{\text{env.}}(t) = 1/(\kappa_{\text{env.}}\rho_{\text{env.}}(t))$ is the photon mean-free path in the envelope whose density is $\rho_{\text{env.}}(t) = M_{\text{env.}}/(4\pi/3 R_{\text{env.}}(t)^3)$. The factor α_{λ} is meant to emulate the spherical geometry of the very extended SN ejecta in our model and the complex opacity effects (temporal and chemical variability) not captured by our simplified model. The $\alpha_{\lambda} = 2/3$ value is only appropriate to planar geometry and when $\lambda_{\text{env.}} \ll R_{\text{env.,}}$ which is not the case here.

3.2. Diffusion in the core

The output luminosity from diffusion in the core is also found using Eq. (3) in Chatzopoulos et al. (2012) for $t > t_{\text{core,sh.}}$. The second term in that equation is the exponential decay expected when pure diffusion controls the luminosity output. The initial value of the output luminosity in this stage is the power output from the envelope at $t = t_{\text{core,sh.}}$. The time $t_{\text{core,sh.}}$ is found when the envelope’s photosphere crosses the core radius; i.e. when $R_{\text{env.,ph.}} = R_{\text{core}}$. Mathematically we solve the following equation $R_{\text{env.,0}} + v_{\text{SN}}t - \alpha_{\lambda}(2/3)\lambda_{\text{env.}} = R_{\text{core,0}} + v_{\text{core}}t$. This introduces another parameter which is the initial size of the core, $R_{\text{core,0}}$ when the QN goes off. For a homologously expanding ejecta this gives us the core’s expansion velocity from $v_{\text{core}} = v_{\text{SN}}(R_{\text{core,0}}/R_{\text{env.,0}})$. The characteristic LC timescale in the core is then $t_{\text{core,d}} = \sqrt{2\kappa_{\text{core}}M_{\text{core}}/(\beta cv_{\text{core}})}$ with κ_{core} the mean opacity in the core.

To summarize, the free parameters in our model can be divided into the following categories: (i) The SN parameters (E_{SN} and M_{WO}); (ii) The QN parameters ($E_{\text{QN}}^{\text{KE}}$ and t_{delay}); (iii) The envelope parameters $E_{\text{env.}}/E_{\text{QN}}^{\text{KE}}$, the envelope mass $M_{\text{env.}}$ and the envelope’s mean opacity $\kappa_{\text{env.}}$; (iv) The core initial radius $R_{\text{core,0}}/R_{\text{env.,0}}$ and its mean opacity κ_{core} ; (v) The parameter α_{λ} related to the photospheric radius.

Figure 2 shows our fit to ASASSN-15lh’s bolometric LC, its photospheric radius and temperature using the parameters given in Table 1. The output luminosity (L_{out} , shown as the solid red line in Figure 2) is first dominated by that from the QN-shocked envelope before switching to the contribution from the core shortly after $t = t_{\text{env.,sh.}} \simeq 6t_{\text{delay}}$. When the envelope’s photosphere crosses the core at $t = t_{\text{core}}$, it becomes transparent to the core and the core’s input power into the envelope ceases. The luminosity then is from pure diffusion in the core declining exponentially as the core cools. For the fit shown here $t_{\text{core}} \simeq 140$ days which is depicted by the vertical thin line in the panels Figure 2.

Shown in the middle panel is the photosphere in the envelope (the blue dashed curve) as it reaches a maximum before it recedes deeper in the envelope first powered by the outer shock then by the slowly contributing inner shock. Eventually, the photosphere in the envelope reaches deep into the core (at $t = t_{\text{core,sh.}}$) at which point in time it disappears leaving place for a new photosphere to propagate inside the core, cooling it (the green dot-dashed curve). The effective photospheric radius ($R_{\text{eff.}}$) is the maximum photospheric radius between the two phases (middle panel). The effective temperature (shown in the lower panel) is derived from the blackbody luminosity as $T_{\text{eff.}} = (L_{\text{out}}/(4\pi\sigma_{\text{SB}}R_{\text{eff.}}^2))^{1/4}$; σ_{SB} is the Stefan-Boltzmann constant. A simultaneous fit of the LC and the photospheric radius required $\alpha_{\lambda} = 1.6$ and better captured the transition between the two photospheres. In reality, the transition from the envelope to the core is more complex and would necessitate numerical simulations to reproduce. Nevertheless, despite the simple approach we adopted here, our model is capable of capturing the general light-curve behavior and the corresponding effective photospheric radius and temperature.

TABLE 1
SAMPLE PARAMETER FITS TO THE LC OF ASASSN-15LH

SN		QN		Envelope			Core	
E_{SN} (ergs)	M_{WO} (M_{\odot})	$E_{\text{QN}}^{\text{KE}}$ (ergs)	t_{delay} (days)	$E_{\text{env.}}/E_{\text{QN}}^{\text{KE}}$	$M_{\text{env.}}$ (M_{\odot})	$\kappa_{\text{env.}}$ ($\text{cm}^2 \text{g}^{-1}$)	$R_{\text{core},0}/R_{\text{env.},0}$	κ_{core} ($\text{cm}^2 \text{g}^{-1}$)
2.5×10^{51}	3.5	1.7×10^{52}	8.5	0.68	1.0	1.2	0.09	2.4

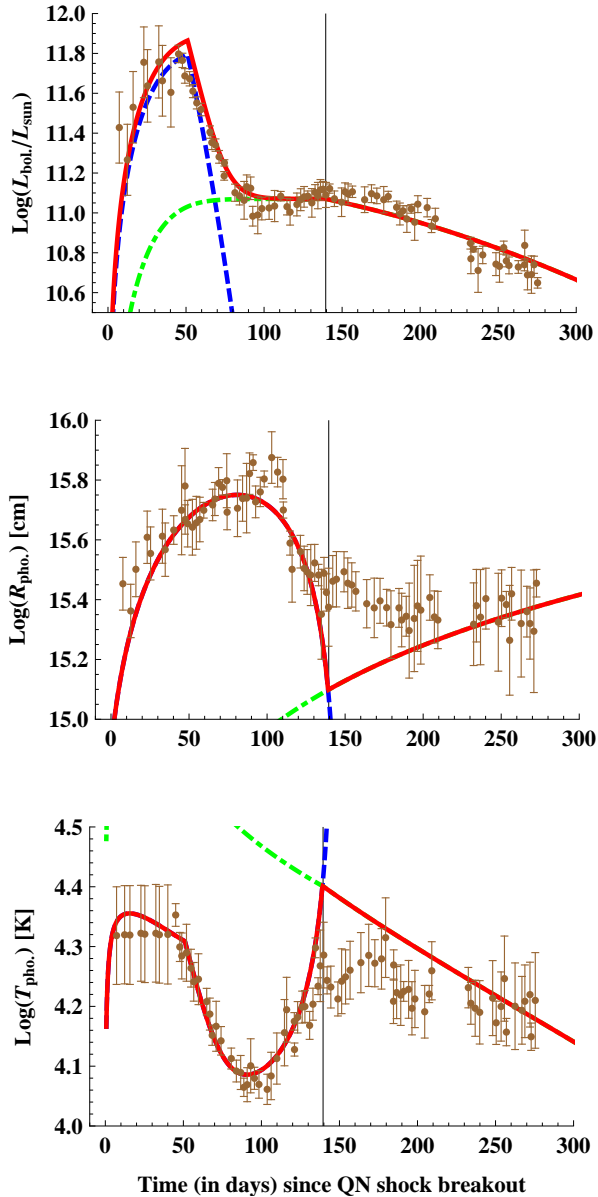


FIG. 2.— The QN model fit (solid red line) to ASASSN-15lh’s bolometric LC (top panel), photospheric radius (middle panel) and photospheric temperature (bottom panel); the data is from Dong et al. (2016) and Brown et al. (2016). The blue dashed (green dot-dashed) curve depicts the envelope’s (core’s) contribution. The vertical line depicts the moment in time when the envelope’s photosphere crosses the core. The time of explosion in our model is 30 days relative to $t = 0$ in the data.

4. DISCUSSION AND CONCLUSION

Here we put forward the idea of a QN occurring inside a homologously expanding, uniform density, SN remnant of a stripped WO star to explain the observed properties

of ASASSN-15lh. For a time delay of ~ 8.5 days between the SN and the QN, the model is capable of reproducing the energetics and the double-peaked light curve of ASASSN-15lh as well as the overall behavior of the photosphere (radius and temperature). The first hump in our model is from the QN shock propagating in the low-density envelope while the second hump is from the slower contribution of the deep hot core to the envelope heating. Below are some features and predictions of our model:

(i) No hydrogen or helium was detected in ASASSN-15lh (Dong et al. 2016) which is expected in our model since the Wolf-Rayet (WO) star has been stripped of both elements prior to the SN explosion;

(ii) If the stripped Wolf-Rayet star experienced a standard SN shock, as we propose here, then oxygen and carbon burning should yield some magnesium, silicon, sulfur and some calcium which we predict may be present (albeit in small quantities) in the spectrum of ASASSN-15lh-like events. The time delay between the SN and the QN means that the QN shock will propagate in a low-density WO remnant (as compared to a SN shock in a stellar envelope) and in principle should not affect the chemical composition of the WO SNR. Contribution from ^{56}Ni decay could in principle be detected later in the LC evolution but this may be too faint particularly if fall-back during the SN was important. The fall-back would help the NS gain enough mass to experience quark deconfinement in its core and undergo a QN explosion. The spectrum will be modelled and simulated elsewhere;

(iii) A nearby ASASSN-15lh-like event may show a precursor, the associated WO-type SN explosion, if the time delay between the SN and QN is long enough to avoid overlap with the brighter peaks. In our model, naturally, the overall shape of the resulting SLSN light-curve should vary from a single hump to a triple hump depending on the time delay between the SN and the QN and the importance of the core’s contribution. We even predict a fourth hump if the QN-shocked ejecta manages to collide with the WO wind or any circumstellar material. Such a late bump would show signatures of hydrogen and helium;

(iv) While the model presented here focuses on a QN in the wake of an WO-type SN, other scenarios involving QNe inside other types of WR stars (e.g. WN and WC) may be possible which should yield similar superluminous events with nevertheless some distinctive spectral features. We note that since WO stars are the rarest amongst WR stars, events such as ASASSN-15lh would be scarce;

(v) The QN leaves behind a QS with a spin-down (SpD) timescale $\tau_{\text{SpD}} \simeq 4 \times 10^7 \text{ s } P_{10}^2 B_{14}^{-2}$ if born with a 10 millisecond period and a typical QS magnetic field of 10^{14} G (e.g. Iwazaki 2005). This gives a spin-down X-ray luminosity $L_X \simeq 5 \times 10^{42} \text{ erg s}^{-1} (1 + t/\tau_{\text{SpD}})^{-2}$. One year after the QN event this would correspond to

$\sim 10^{42}$ erg s $^{-1}$ which seems to agree with the detected persistent X-ray emission in ASASSN-15lh (Margutti et al. 2016). The current QS period exceeds 10 ms but spin-down power could still affect the late evolution of ASASSN-15lh LC.

(vi) Our model applies to any progenitor star (O-stars, luminous blue variables, Wolf-Rayet stars, etc.) if it is massive enough to go SN and form a heavy NS but not too massive to go directly to a black hole. This is the unifying scheme between SLSNe, as first suggested in Ouyed, Koning & Leahy (2013) and Ouyed & Leahy

(2013), where the Type (I or II) of the SLSN defines the chemical composition of the SN progenitor. We reiterate, and argue again, that H-poor SLSNe would occur in higher-metallicity environment (i.e. with higher stellar mass loss-rates) while low-metallicity progenitors would lose less mass and should be linked to SLSN-II if a QN goes off in their wake.

This work is funded by the Natural Sciences and Engineering Research Council of Canada.

REFERENCES

- Arnett, W. D. 1980, *ApJ*, 237, 541
 Arnett, W. D. 1982, *ApJ*, 253, 785
 Barlow, M. J., & Hummer, D. G. 1982, in *Wolf-Rayet Stars: Observations, Physics, Evolution*, eds. C. W. H. De Loore, & A. J. Willis, IAU Symp., 99, 387
 Bodmer, A. R. 1971, *Phys. Rev. D*, 4, 1601
 Brown, P. J., Yang, Y., Cooke, J., et al. 2016, *ApJ*, 828, 3
 Chatzopoulos, E., Wheeler, J. C., & Vinko, J. 2012, *ApJ*, 746, 121
 Chatzopoulos, E., van Rossum, D. R., Craig, W. J., Whalen, D. J., Smidt, J., & Wiggins, B. 2015, *ApJ*, 799, 18, 1410.0039
 Chatzopoulos, E., Wheeler, J. C., Vinko, J., Nagy, A. P., Wiggins, B. K., & Even, W. P. 2016, *ArXiv e-prints*
 Cheng, K. S., & Dai, Z. G. 1996, *Physical Review Letters*, 77, 1210
 Dai, Z., Peng, Q., & Lu, T. 1995, *ApJ*, 440, 815
 Dai, Z. G., Wang, S. Q., Wang, J. S., Wang, L. J., & Yu, Y. W. 2016, *ApJ*, 817, 132
 Dessart, L., Audit, E., & Hillier, D. J. 2015, *MNRAS*, 449, 4304, 1503.05463
 Dexter, J. & Kasen, D. 2013, *ApJ*, 772, 30
 Dong, S., Shappee, B. J., Prieto, J. L., et al. 2016, *Science*, 351, 257
 Drago, A., & Pagliara, G. 2015a, *Phys. Rev. C*, 92, 045801
 Drago, A., & Pagliara, G. 2015b, *arXiv:1509.02134*
 Furusawa, S., Sanada, T., & Yamada, S. 2015a, *arXiv:1511.08148*
 Furusawa, S., Sanada, T., & Yamada, S. 2015b, *arXiv:1511.08153*
 Gal-Yam, A. 2012, *Sci*, 337, 927
 Gilkis, A., Soker, N., & Papish, O. 2016, *ApJ*, 826, 178
 Herzog, M., & Röpke, F. K. 2011, *Phys. Rev. D*, 84, 083002
 Horvath, J. E. & Benvenuto, O. G. 1988, *Phys. Lett. B*, 213, 516
 Inserra, C., Smartt, S. J., Jerkstrand, A., et al. 2013, *ApJ*, 770, 128
 Iwazaki, A. 2005, *Phys. Rev. D*, 72, 114003
 Jaikumar, P., Meyer, B. S., Otsuki, K., & Ouyed, R. 2007, *A&A*, 471, 227
 Kasen, D., & Bildsten, L. 2010, *ApJ*, 717, 245
 Keränen, P., Ouyed, R., & Jaikumar, P. 2005, *ApJ*, 618, 485
 Kostka, M., Koning, N., Leahy, D., Ouyed, R., & Steffen, W. 2014a, *Revista Mexicana de Astronomía y Astrofísica*, 50, 167
 Kostka, M., Koning, N., Shand, Z., Ouyed, R., & Jaikumar, P. 2014b, *A&A*, 568, A97
 Kozyreva, A., & Blinnikov, S. 2015, *MNRAS*, 454, 4357, 1510.00439
 Leahy, D., & Ouyed, R. 2008, *MNRAS*, 387, 1193
 Leloudas, G., Fraser, M., Stone, N. C., et al. 2016, *arXiv:1609.02927*
 Margutti, R., Metzger, B. D., Chornock, R., et al. 2016, *arXiv:1610.01632*
 Nicholl, M., Smartt, S. J., Jerkstrand, A., et al. 2014, *MNRAS*, 444, 2096
 Moriya, T. J., Liu, Z.-W., Mackey, J., Chen, T.-W., & Langer, N. 2015, *A&A*, 584, L5
 Niebergal, B., Ouyed, R., & Jaikumar, P. 2010, *Phys. Rev. C*, 82, 062801
 Ouyed, R., Dey, J., & Dey, M. 2002, *A&A*, 390, L39
 Ouyed, R., Rapp, R., & Vogt, C. 2005, *ApJ*, 632, 1001
 Ouyed, R., & Leahy, D. 2009, *ApJ*, 696, 562
 Ouyed, R., Niebergal, B., & Jaikumar, P. 2009, “Predictions for signatures of the quark-nova in superluminous supernovae” in *Proceedings of the Compact Stars in the QCD Phase Diagram II*, <http://vega.bac.pku.edu.cn/rxxu/csqcqcd.htm> [arXiv:0911.5424]
 Ouyed, R., Kostka, M., Koning, N., Leahy, D. A., & Steffen, W. 2012, *MNRAS*, 423, 1652
 Ouyed, R., Niebergal, B., & Jaikumar, P. 2013, “Explosive Combustion of a NS into a QS: the non-premixed scenario” in *Proceedings of the Compact Stars in the QCD Phase Diagram III*, <http://www.slac.stanford.edu/econf/C121212/> [arXiv:1304.8048]
 Ouyed, R., Koning, N., & Leahy, D. 2013, *Research in Astronomy and Astrophysics*, 13, 1463-1470
 Ouyed, R., & Leahy, D. 2013, *Research in Astronomy and Astrophysics*, 13, 1202-1206
 Ouyed, R., Leahy, D., & Koning, N. 2015a, *MNRAS*, 454, 2353
 Ouyed, R., Leahy, D., & Koning, N. 2015b, *ApJ*, 809, 142
 Ouyed, R., Leahy, D., & Koning, N. 2016, *ApJ*, 818, 77
 Pagliara, G., Herzog, M., Röpke, F. K. 2013, *Phys. Rev. D*, 87, 103007
 Piro, A. L. 2015, *ApJ*, 808, L51
 Pastorello, A., Smartt, S. J., Botticella, M. T., et al. 2010, *ApJ*, 724, L16
 Quimby, R. M., Kulkarni, S. R., Kasliwal, M. M., et al. 2011, *Nature*, 474, 487
 Sorokina, E., Blinnikov, S., Nomoto, K., Quimby, R., & Tolstov, A. 2015, *arXiv:1510.00834*
 Vogt, C., Rapp, R., & Ouyed, R. 2004, *Nuclear Physics A*, 735, 543
 Wang, S. Q., Liu, L. D., Dai, Z. G., Wang, L. J., & Wu, X. F. 2015, *arXiv:1509.05543*
 Weber, F. 2005, *Progress in Particle and Nuclear Physics*, 54, 193
 Witten, E. 1984, *Phys. Rev. D*, 30, 272
 Woosley, S. 2010, *ApJ*, 719, L204